

Copyright © 1984, by the author(s).  
All rights reserved.

Permission to make digital or hard copies of all or part of this work for personal or classroom use is granted without fee provided that copies are not made or distributed for profit or commercial advantage and that copies bear this notice and the full citation on the first page. To copy otherwise, to republish, to post on servers or to redistribute to lists, requires prior specific permission.

**INVARIANT DISTRIBUTION ON STRANGE ATTRACTORS  
IN HIGHLY DISSIPATIVE SYSTEMS**

**by**

**K. Y. Tsang and M. A. Lieberman**

**Memorandum No. UCB/ERL M84/13**

**4 January 1984**

**ELECTRONICS RESEARCH LABORATORY**

**College of Engineering  
University of California, Berkeley  
94720**

INVARIANT DISTRIBUTION ON STRANGE ATTRACTORS IN HIGHLY  
DISSIPATIVE SYSTEMS

by

Kwok Yeung Tsang and M. A. Lieberman

Department of Electrical Engineering and Computer Sciences  
and the Electronics Research Laboratory  
University of California, Berkeley, CA 94720

ABSTRACT

We obtain analytically by an iterative procedure the equilibrium invariant distribution for a class of strange attractors in highly dissipative systems. The zeroth order distribution is found by solving the phase-averaged Markov equation. Repeated iterations over the map yield the higher order distributions that reveal successively finer structures. The analytical results have been compared quantitatively to numerical results for the Zaslavskii map.

We have previously developed an iterative procedure to determine analytically the equilibrium invariant distributions on strange attractors in dissipative systems [1]. The initial distribution for the iteration procedure was chosen to be the solution of the appropriate phase-averaged Fokker-Planck equation. This choice gave good results for weakly dissipative systems, but was shown to be invalid for highly dissipative systems. Here we extend the procedure to highly dissipative systems, by developing a direct solution of the phase-averaged Markov equation as the initial distribution for subsequent iteration.

The class of dissipative systems we consider is represented by an invertible perturbed twist map

$$y_{n+1} = y_n + \varepsilon F(x_n, y_{n+1}) , \quad (1a)$$

$$x_{n+1} = x_n + A(y_{n+1}) + \varepsilon G(x_n, y_{n+1}). \quad (1b)$$

Here  $F$  and  $G$  are periodic in  $x$  with period  $2\pi$ , and  $\underline{z} = (x, y)$  are the angle-action variables of the unperturbed ( $\varepsilon=0$ ) Hamiltonian system.

We suppose that for some  $\varepsilon$  a strange attractor exists with a basin of attraction  $B$ . We construct by successive approximations the equilibrium invariant distribution  $f(x, y)$  for the attractor. This distribution satisfies the conditions

$$f(x, y) = Tf(x, y) , \quad (2)$$

$$\frac{1}{2\pi} \int_B f dx dy = 1 , \quad (3)$$

where  $T$  is the mapping, extended to act on distributions. Although there are many invariant distributions for an attractor, a particular one (the equilibrium distribution) is singled out by the fact that the time average over almost any orbit in  $B$  is equal to the ensemble average for this distribution.

The method proceeds from the coarse scaled features of  $f$  to the fine scaled. Previously, we found a phase-averaged invariant distribution  $\bar{f}(y)$ , by assuming that  $\bar{f}(y, n)$  evolves with the "time" (iteration number)  $n$  as a Markov

process in  $y$  alone,

$$\bar{f}(y, n) = \int \bar{f}(y - \Delta y, 0) P(y - \Delta y, n | \Delta y) d(\Delta y) , \quad (4)$$

where  $P(y, n | \Delta y)$  is the probability density that an initial ensemble of phase space points at  $y$  suffers an increment  $\Delta y$  after a time  $n$ .

Making the assumption that

$$1 \ll n \ll \left( \frac{\varepsilon F_{\max}}{f} \frac{df}{dy} \right)^2 , \quad (5)$$

the equilibrium invariant distribution was then determined from a Fokker-Planck equation in the action alone:

$$\frac{\partial \bar{f}}{\partial n} = - \frac{\partial}{\partial y} (B \bar{f}) + \frac{1}{2} \frac{\partial^2}{\partial y^2} (D \bar{f}) , \quad (6)$$

where

$$B(y) = \frac{1}{2\pi} \int_0^{2\pi} dx (\Delta y) \quad (7)$$

and

$$D(y) = \frac{1}{2\pi} \int_0^{2\pi} dx (\Delta y)^2 \quad (8)$$

are respectively the friction and diffusion coefficients under the random phase assumption, and  $\Delta y = \varepsilon F(x, y)$  from (1a). When the Fokker-Planck equation is a good approximation for the Markov process, then the equilibrium solution obtained from (6) is a good initial approximation for the invariant distribution:

$$f^{(0)}(x, y) = \bar{f}(y) . \quad (9)$$

To find successively higher order approximations, we iterate (9) by the map. Letting  $\underline{z}' = (x', y')$  be the pre-image of  $\underline{z} = (x, y)$ , the  $i$  and  $i+1$  approximations are related by

$$f^{(i+1)}(x, y) dx dy = f^{(i)}(x', y') dx' dy' , \quad (10)$$

which yields

$$f^{(i+1)}(\underline{z}) = J f^{(i)}(\underline{z}'(\underline{z})) , \quad (11)$$

where

$$J(T^{-1}\underline{z}) = \left| \frac{\partial(x', y')}{\partial(x, y)} \right| \quad (12)$$

is the Jacobian of the inverse map

$$T^{-1}\underline{z} = \underline{z}'(\underline{z}) . \quad (13)$$

By repeatedly applying (11) we obtain the  $n$ th order approximation

$$f^{(n)}(\underline{z}) = f^{(0)}(T^{-n}\underline{z}) \prod_{i=1}^n J(T^{-i}\underline{z}) . \quad (14)$$

The condition (5) for validity of the Fokker-Planck equation (6) is not satisfied when the Jacobian  $J$  of the inverse map much exceeds unity. In previous work [1], we studied several cases where the dissipation was small

$$J - 1 \ll 1$$

and condition (5) was satisfied. These cases all showed good agreement between analytical and numerical results, thus verifying the validity of the Fokker-Planck initial choice. We also studied a case where the dissipation was large ( $J = 10$ ). We noted that the Fokker-Planck solution did not agree well with numerical calculations in this case, and that it would seem better to determine the zeroth order distribution by direct solution of the Markov process (4). In this letter we present such a procedure, leading to a more accurate determination of the equilibrium invariant distribution when the Fokker-Planck theory breaks down.

In the steady state, the Markov equation (4) can be written in the form

$$\bar{f}(y) = \int \bar{f}(y') P(y | y') dy' \quad (15)$$

where  $P(y|y')$  is the probability density that an initial ensemble of phase space points at  $y'$  makes a transition to  $y$  after one iteration of equations (1).

Such an  $\bar{f}$  is difficult to find analytically, but may be obtained by an iterative procedure:

$$\bar{f}_{j+1}(y) = \int \bar{f}_j(y') P(y|y') dy' . \quad (16)$$

As  $j$  becomes large,  $\bar{f}_j$  will converge to an  $\bar{f}$  satisfying (15) for almost all  $\bar{f}_0$ .

If we choose a simple and reasonably accurate  $\bar{f}_0$ ,  $\bar{f}_1$  can be obtained analytically instead of numerically. Such an  $\bar{f}_1$  may be near enough to  $\bar{f}$  to serve as the initial choice  $f^{(0)}$  for successively higher order approximations to the equilibrium invariant distribution, obtained from (14). To apply this procedure, we choose as  $\bar{f}_0$  the distribution that is uniform over the smallest rectangular region of the phase space  $(x,y)$  that maps into itself.

We apply the above procedure to the Zaslavskii map [2,3]

$$y = (1-\delta)y' + k \sin 2\pi x' , \quad (17a)$$

$$x = x' + y \mod 1 . \quad (17b)$$

The Jacobian of the inverse map is  $J = (1-\delta)^{-1}$ . We assume  $J \gg 1$  and choose  $\bar{f}_0(y')$  uniform in  $y'$  for  $|y'| < y$ . Here  $y$  is the smallest positive  $y'$  such that  $y'$  exceeds  $y(x',y')$  for all  $x'$ . From (17a), we obtain

$$y = k/\delta . \quad (18)$$

Consequently, we have

$$\bar{f}_0(y) \propto [H(y+k/\delta) - H(y-k/\delta)] , \quad (19)$$

where  $H$  is the unit step function.

To obtain  $P(y|y')$ , we consider a thin strip in the  $(x',y')$  plane  $0 < x' \leq 1$ ,  $y_0 < y' < y_0 + \Delta$ , where  $\Delta \ll k$ . From (17a), this strip maps to an arcsinoidal strip in the  $(x',y)$  plane having as borders the two curves

$$x_1'(y) = \frac{1}{2\pi} \sin^{-1} \left[ \frac{y - (1-\delta)y_0}{k} \right],$$

$$x_2'(y) = \frac{1}{2\pi} \sin^{-1} \left[ \frac{y - (1-\delta)(y_0 + \Delta)}{k} \right].$$

The transition probability  $P(y | y')$  is proportional to  $|x_1' - x_2'| \propto dx'/dy$ .

We therefore find

$$P(y | y') = \sigma \left[ \frac{y - (1-\delta)y'}{k} \right], \quad (20)$$

where

$$\begin{aligned} \sigma(\xi) &\propto \frac{d}{d\xi} \sin^{-1} \xi, \quad |\xi| \leq 1; \\ &= 0, \quad |\xi| > 1. \end{aligned} \quad (21)$$

Therefore we have, from (19) and (20),

$$\begin{aligned} \bar{f}_1(y) &= \int_{-\infty}^{\infty} \bar{f}_0(y') P(y | y') dy' \\ &\propto \int_{\frac{y-k}{1-\delta}}^{\frac{y+k}{1-\delta}} dy' \left[ H(y + \frac{k}{\delta}) - H(y - \frac{k}{\delta}) \right] \left( -\frac{d}{dy'} \right) \sin^{-1} \left[ \frac{y - (1-\delta)y'}{k} \right]. \end{aligned}$$

Integrating by parts, we obtain

$$\bar{f}_1(y) \propto g(y - \frac{\eta}{k}) - g(y + \frac{\eta}{k}), \quad (22)$$

where

$$g(\chi) = \begin{cases} 0, \chi > 1; \\ \frac{1}{2} - \frac{1}{\pi} \sin^{-1} \chi, \quad |\chi| \leq 1; \\ 0, \chi < -1; \end{cases} \quad (23)$$

and

$$\eta = (\delta^{-1} - 1)k \quad . \quad (24)$$

Normalizing as in (3), we have

$$\bar{f}_1(y) = \frac{1}{2\eta} \left[ g\left(\frac{y-\eta}{k}\right) - g\left(\frac{y+\eta}{k}\right) \right] \quad . \quad (25)$$

To verify the validity of this  $\bar{f}_1$ , we choose  $k = 1.4$  and  $\delta = 0.9$  ( $J=10$ ). In Fig. 1, the analytical distribution  $\bar{f}_1$  in (25) is compared with the numerical result obtained from  $10^5$  iterations of a single initial condition. The agreement is good, and  $\bar{f}_1$  is a much better estimate of the phase-averaged distribution than the Fokker-Planck distribution (see Fig. 1).

$$\bar{f}_{FP} = \left( \frac{2\delta}{\pi} \right)^{1/2} \exp(-2\delta y^2/k^2) \quad , \quad (26)$$

obtained by solving (6)-(8) in the steady state [1].

In principle,  $\bar{f}_0, \bar{f}_1, \bar{f}_2, \dots$ , form a sequence converging to the solution  $\bar{f}$  satisfying (15). However, it is difficult to determine  $\bar{f}_2, \bar{f}_3$ , etc. analytically, and we resort to numerical calculation. We divide the range  $|y| < 2$  into 100 equal intervals and use (25) in (16) to determine  $\bar{f}_2$ .

The distribution  $\bar{f}_2$  qualitatively appears to be very close to  $\bar{f}_1$ . However, to compare two distributions quantitatively, we must introduce a measure of resemblance between them. We use the mean square hyperbolic deviation  $E^2$ , introduced in reference 1, as the measure of resemblance between the analytical and numerical distributions. For two distributions  $f$  and  $g$ , each having  $N$  occupations in a domain that has been partitioned into  $K$  cells, we write

$$E^2 = \frac{4}{N} \sum_{j=1}^K (\sqrt{f_j} - \sqrt{g_j})^2 \quad , \quad (27)$$

where  $f_j \geq 0$  and  $g_j \geq 0$  are the number of occupations in cell  $j$ . Introducing the mean occupation number  $\mu = N/K$ , we see that  $E$  represents the (hyper-

bolic rms) number of standard deviations  $\sqrt{\mu}$  by which  $f$  and  $g$  differ. Two distributions closely resemble each other if  $E^2 \ll 1$ .

The comparison of an analytical with a numerical distribution is limited by noise (Poisson fluctuations) in the latter. If an analytical and a numerical distribution agree exactly (except that the numerical distribution is corrupted by noise), then the best agreement we can expect is  $E^2 = E_R^2(\mu) > 0$ . A graph of  $E_R^2(\mu)$  was given in reference 1; here, we need note only that for  $\mu \gg 1$ ,  $E_R^2 = \mu^{-1}$ .

To verify quantitatively that  $\bar{f}_2$  and  $\bar{f}_3$  are not much better than  $\bar{f}_1$  when compared to the numerically determined distribution, we divide the range  $|y| \leq 2$  into  $K = 100$  intervals each having  $\Delta y = 0.02$ . Using  $N = 10^5$  iterations of the map to determine the numerical distribution,  $E_R^2 = 0.001$ . The deviations  $E^2$  between  $\bar{f}_1$ ,  $\bar{f}_2$ , and  $\bar{f}_3$  and the numerically determined distribution are found to be 0.107, 0.103, and 0.104 respectively. Thus  $\bar{f}_2$  and  $\bar{f}_3$  are no improvement over  $\bar{f}_1$ , and we can choose  $\bar{f}_1(y)$  given by (25) as the initial guess  $f^{(0)}(x,y)$  in (14).

Figure 2a shows the numerically determined distribution obtained from  $10^5$  iterations of the Zaslavskii map (17) for a single initial condition. The  $(x,y)$  plane has been partitioned into  $100 \times 100$  cells, and the number inside each cell (not readily seen) is a logarithmic measure of the number of occupations.

Figures 2b and 2c show the corresponding analytical results for  $f^{(1)}$  and  $f^{(2)}$  obtained from (14). To see that they resemble the numerical distribution more closely than those obtained from the Fokker-Planck distribution (26) do, we refer to the results in Table 1. In the region  $|y| \leq 2$ ,  $f^{(1)}$  obtained by using (25) has  $E^2 = 0.60$ , which is considerably smaller than  $E^2 = 1.02$  obtained by using the Fokker-Planck result (26). Iterating yet again to obtain  $f^{(2)}$ , we see that either (25) or (26) yields  $E^2 = 0.2$ . However, if we focus on a smaller

region of the attractor, we again see a difference.

Figure 3a is an enlargement of a small region for the numerical calculation shown in Fig. 2a. Here we have chosen a single initial condition iterated  $10^8$  times, for a total of 37326 occupations of the map. In Fig. 3b,  $f^{(2)}$  is plotted using (25) as the initial guess for the same region as the numerical plot in Fig. 3a. We see not only that the structures look similar, but also from Table 1 that  $E^2$  thus obtained is smaller than that obtained using the Fokker-Planck initial guess.

Continuing to examine finer structures, we go to higher orders. In Fig. 4a, the central region in Fig. 3b is expanded, and  $f^{(3)}$  is plotted. In Fig. 4b, the central region in Fig. 4a is expanded again and  $f^{(4)}$  is plotted. Both  $f^{(3)}$  and  $f^{(4)}$  look similar to  $f^{(2)}$ , displaying the rescaling properties typically seen for strange attractors. When comparing the distributions in Figs. 4a and 4b with Fig. 3a, the corresponding values of  $E^2$  are again smaller than those obtained [1] using the Fokker-Planck initial guess.

In conclusion, the approximate equilibrium invariant distribution on a strange attractor for a two-dimensional perturbed twist map can be determined analytically by iterating a certain phase-averaged distribution over the map. Previous work [1] for small dissipation showed that this phase-averaged distribution is the stationary solution of the appropriate Fokker-Planck equation for the map. The theory has been extended here to large dissipation, for which the phase-averaged distribution is determined directly from the phase-averaged Markov equation, starting with a uniform distribution on an appropriately chosen simple region of the map.

5  
1  
1

#### ACKNOWLEDGEMENT

We gratefully acknowledge that this research was sponsored by the Office of Naval Research Contract N00014-79-C-0674 and the National Science Foundation Grant ECS-8104561.

### References

- [1] Kwok Yeung Tsang and M. A. Lieberman, Physica D (1983), in press.
- [2] R. V. Jensen and C. R. Oberman, Physica 4D (1982) 183.
- [3] G. M. Zaslavskii, Phys. Lett. 69A (1978) 45.

Table 1: Comparison of Theory and Numerical Results for the Zaslavskii Map with  $k = 1.4$ ,  $\delta = 0.9$ , and  $K = 10^4$ .

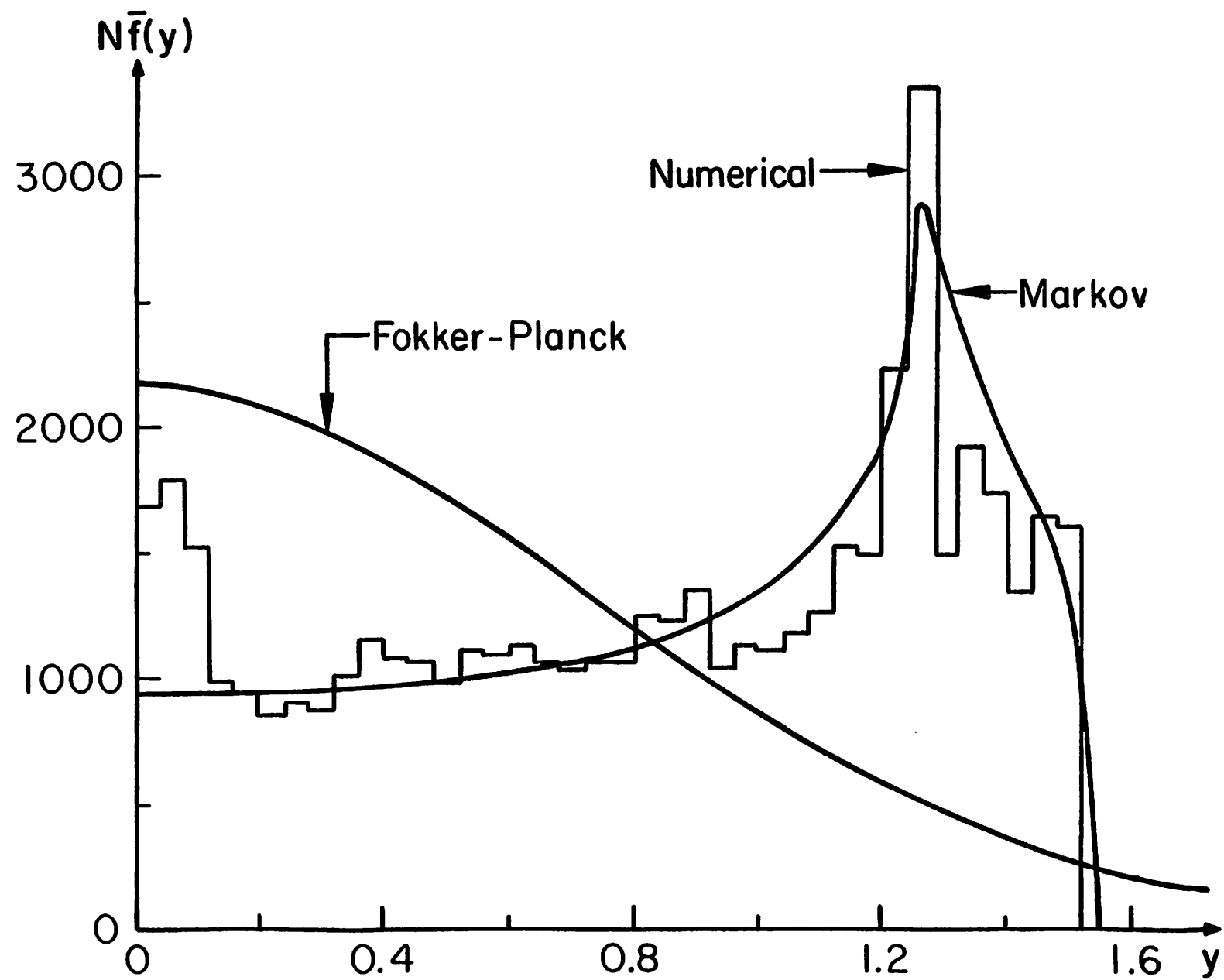
| region                   | $ y  \leq 2$ |        |        | $ y  < 0.06$ | $ y  \leq 0.000775$ | $ y  \leq 0.00001$ |
|--------------------------|--------------|--------|--------|--------------|---------------------|--------------------|
| order                    | $f(0)$       | $f(1)$ | $f(2)$ | $f(2)$       | $f(3)$              | $f(4)$             |
| occupations N            | 100,000      |        |        | 37,326       |                     |                    |
| $E_R^2$                  | 0.11         |        |        | 0.35         |                     |                    |
| $f^{(0)} = \bar{f}_1$    | 5.03         | 0.60   | 0.20   | 0.79         | *0.79               | *0.86              |
| $f^{(0)} = \bar{f}_{FP}$ | 5.31         | 1.02   | 0.20   | 0.92         | **0.92              | **0.98             |

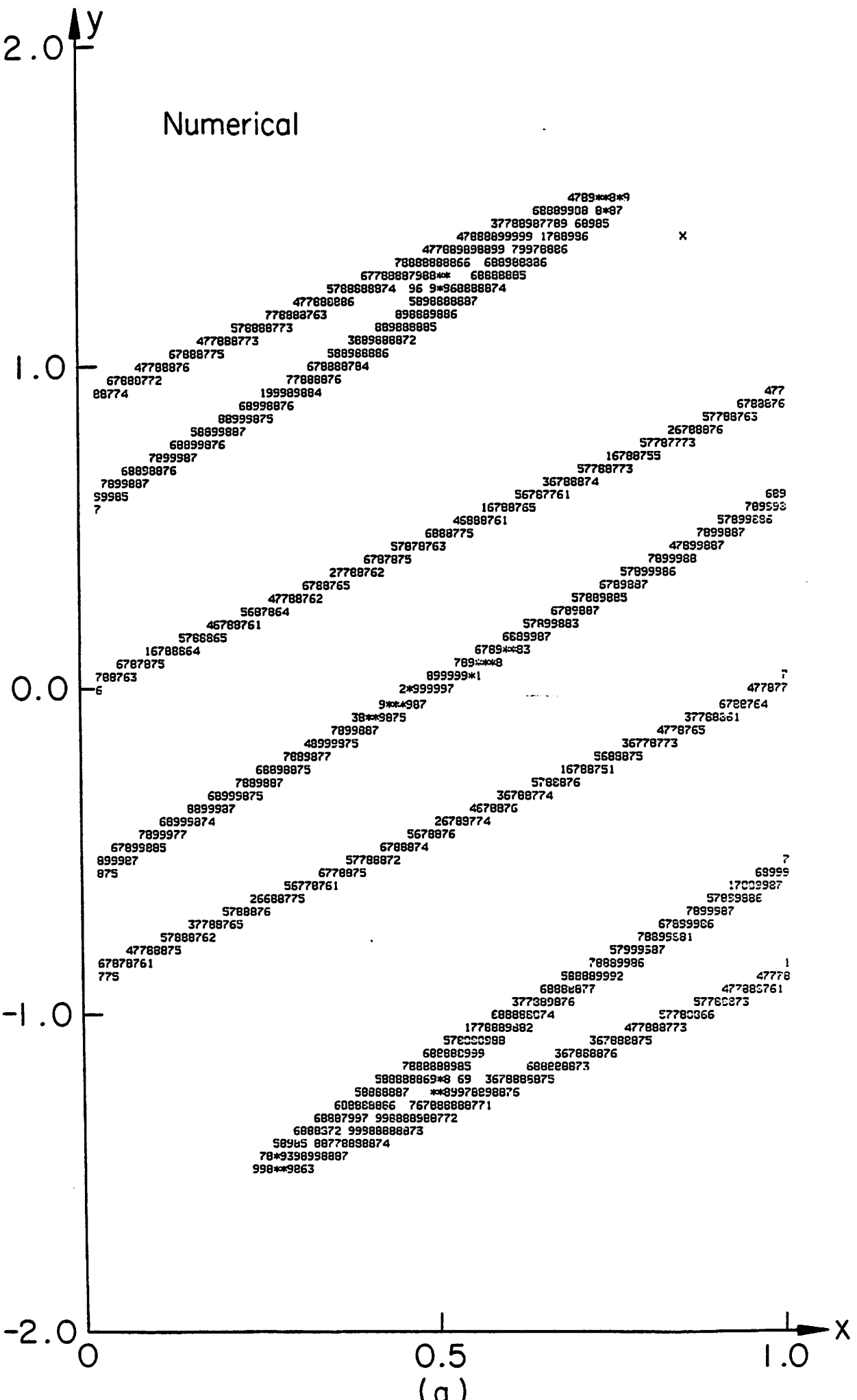
\* Rescaling  $|y| \leq 0.000775$  to  $|y| \leq 0.06$ .

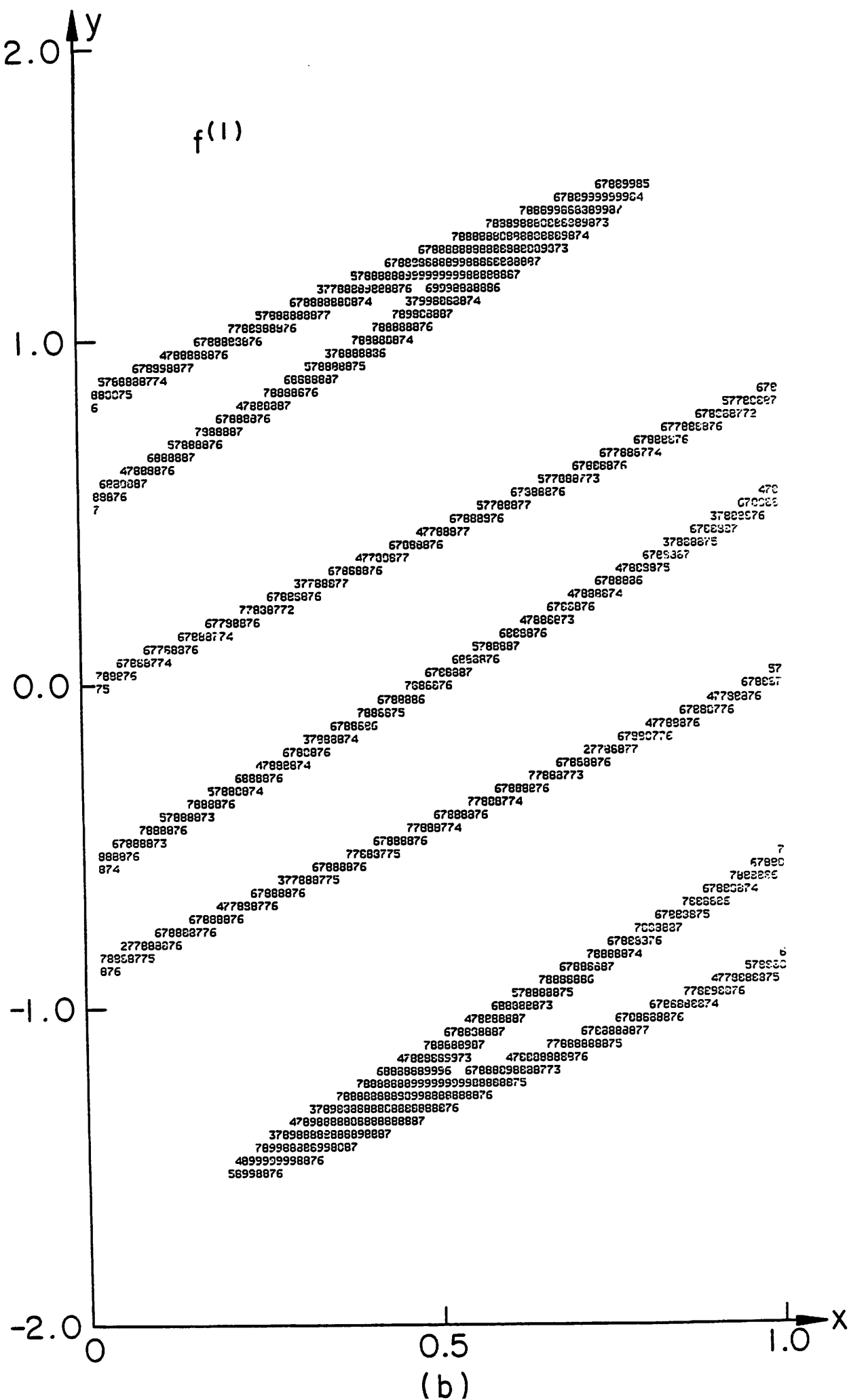
\*\* Rescaling  $|y| \leq 0.00001$  to  $|y| \leq 0.06$ .

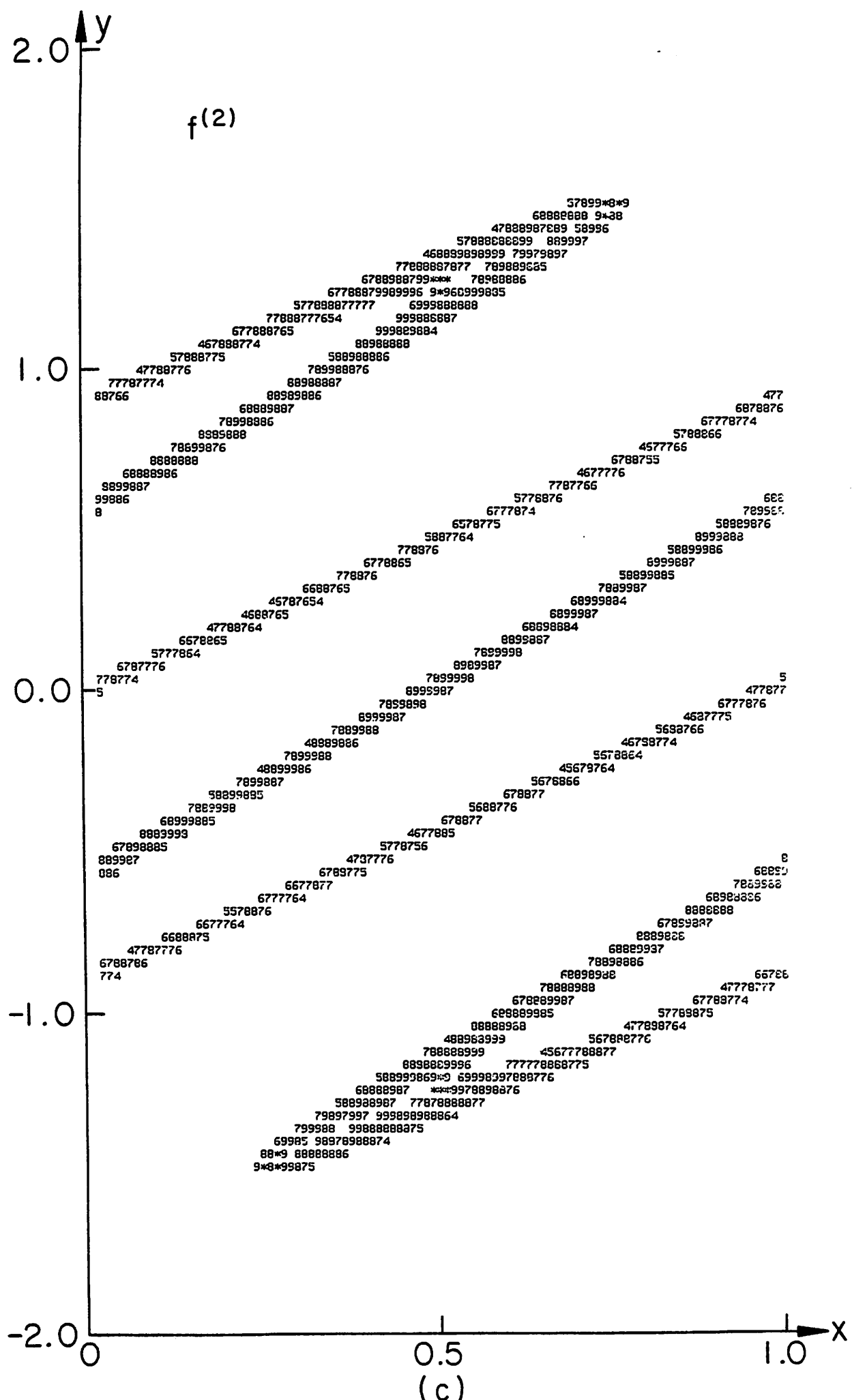
## FIGURE CAPTIONS

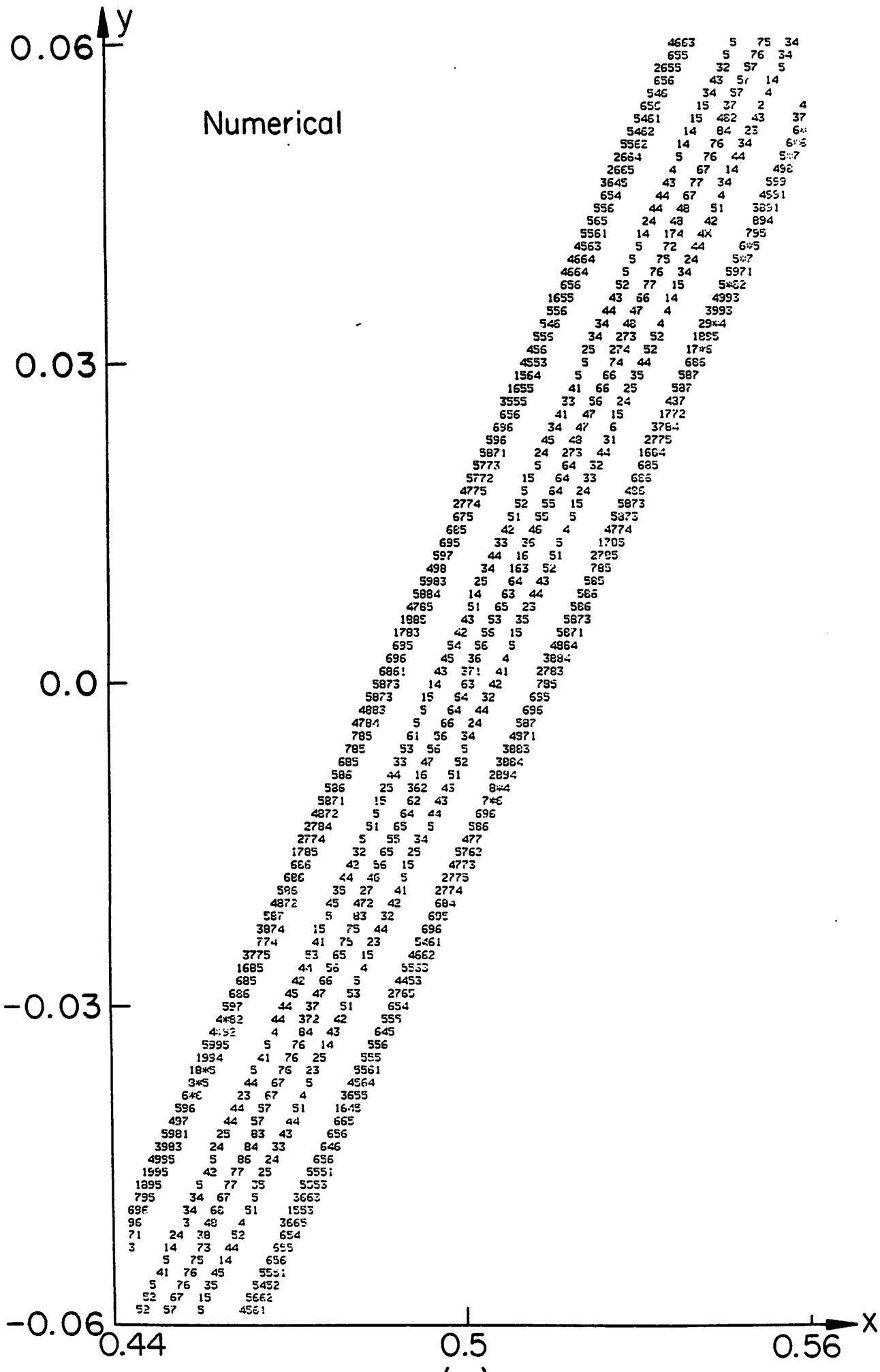
- Fig. 1. Comparison of the Markov and Fokker-Planck analytical distributions with the numerical phase-averaged distributions for the Zaslavskii map with  $k = 1.4$ ,  $\delta = 0.9$ , and  $N = 10^5$ .
- Fig. 2. Phase space  $y-x$  for the Zaslavskii map with  $k = 1.4$  and  $\delta = 0.9$ , in the range  $-2 \leq y \leq 2$ . (a) Numerically obtained from one initial condition ( $x$ ) with 100,000 collisions; (b) Analytically obtained first order result  $f^{(1)}(x,y)$  using the Markov initial choice  $\bar{f}_1$ ; (c) Analytically obtained second order result  $f^{(2)}(x,y)$  using the Markov choice  $\bar{f}_1$ .
- Fig. 3. Phase space  $y-x$  for the Zaslavskii map with  $k = 1.4$  and  $\delta = 0.9$ , in the range  $0.44 \leq x \leq 0.56$ ,  $-.06 \leq y \leq .06$ . (a) Numerically obtained from one initial condition with 1,000,000 collisions, of which 37326 occupations are shown; (b) Analytically obtained second order result  $f^{(2)}(x,y)$  using the Markov choice  $\bar{f}_1$ .
- Fig. 4. Successive magnifications of the analytical result in Fig. 3b showing (a) third order structure and (b) fourth order structure.











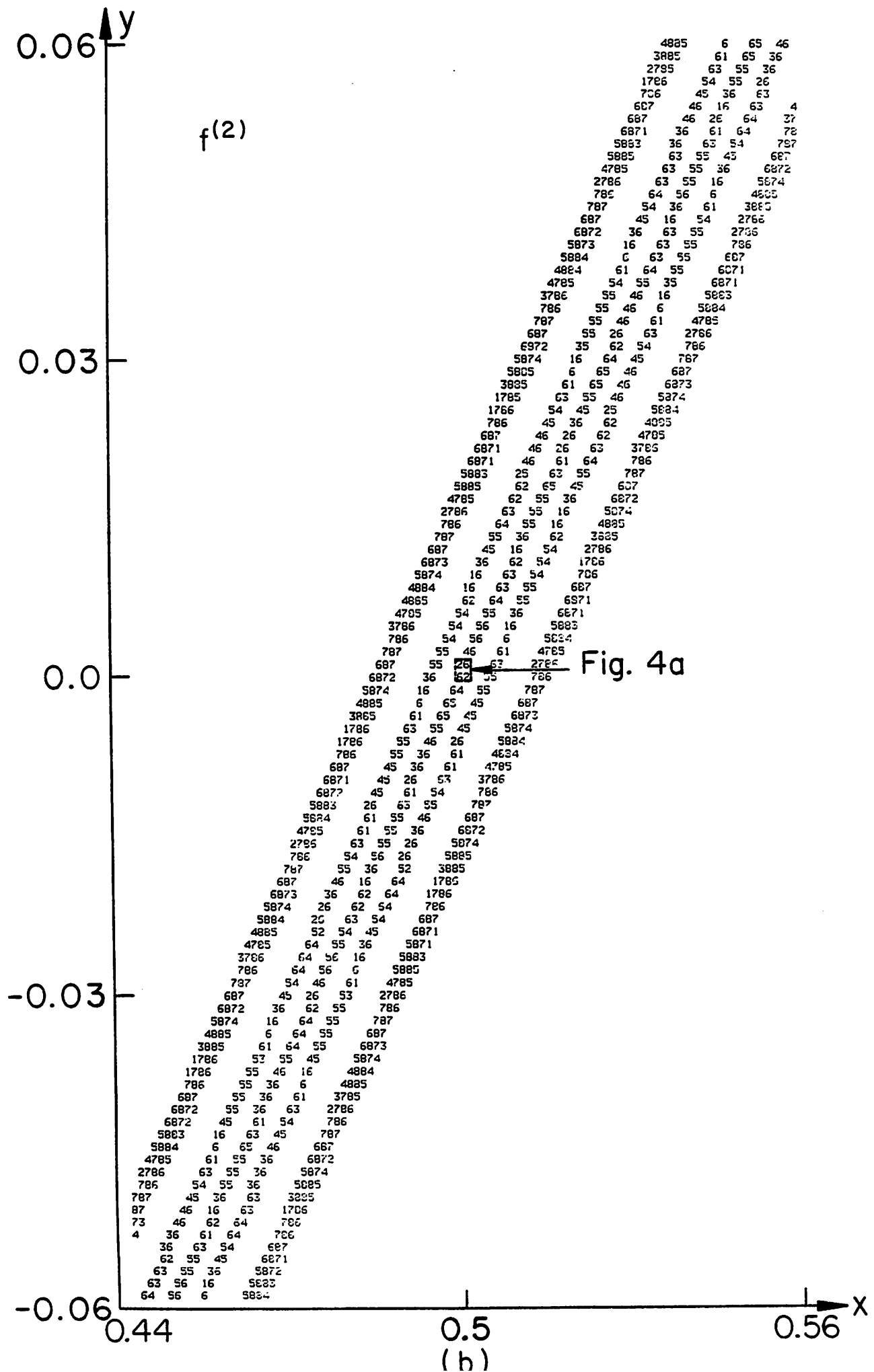
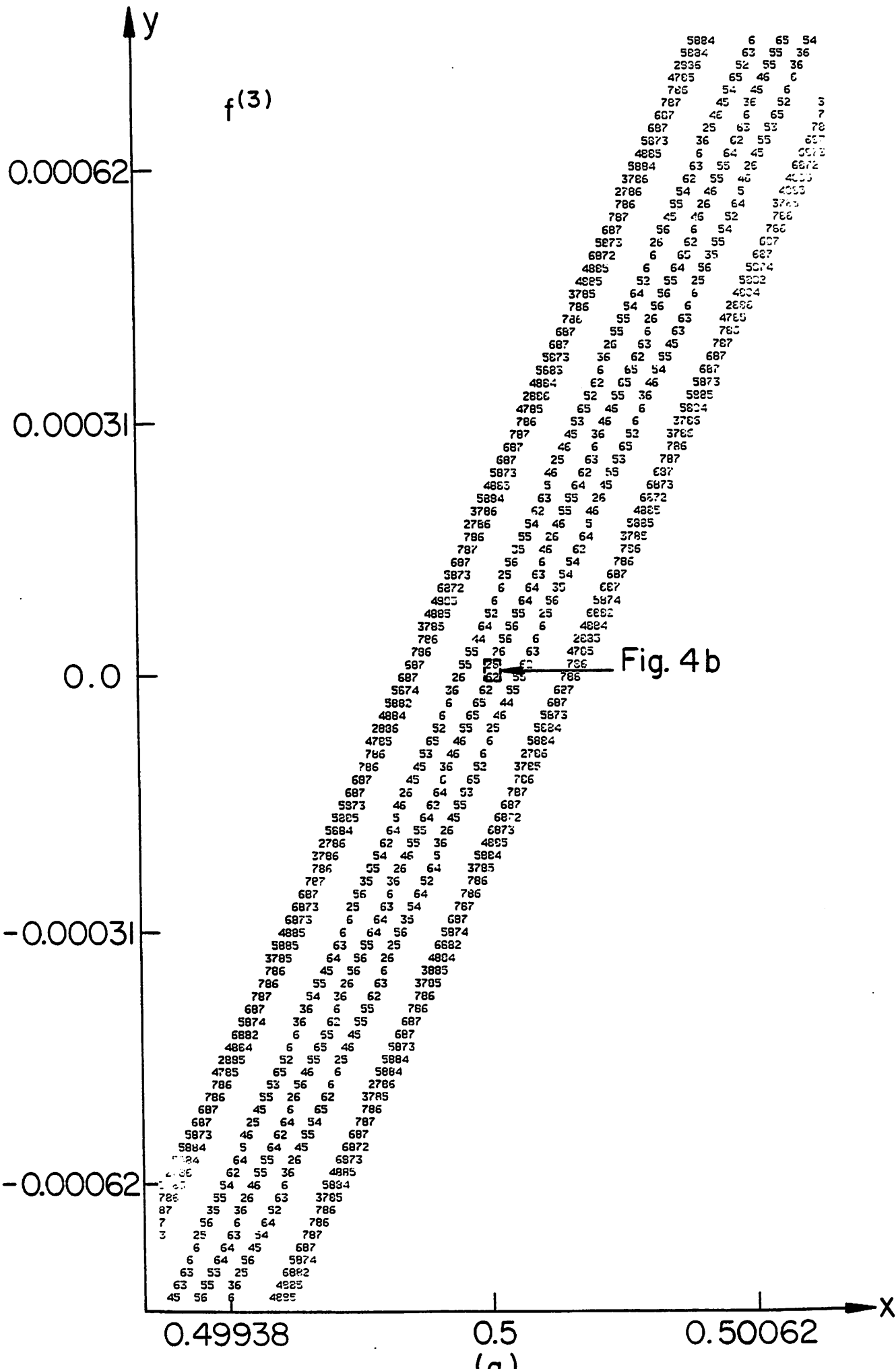
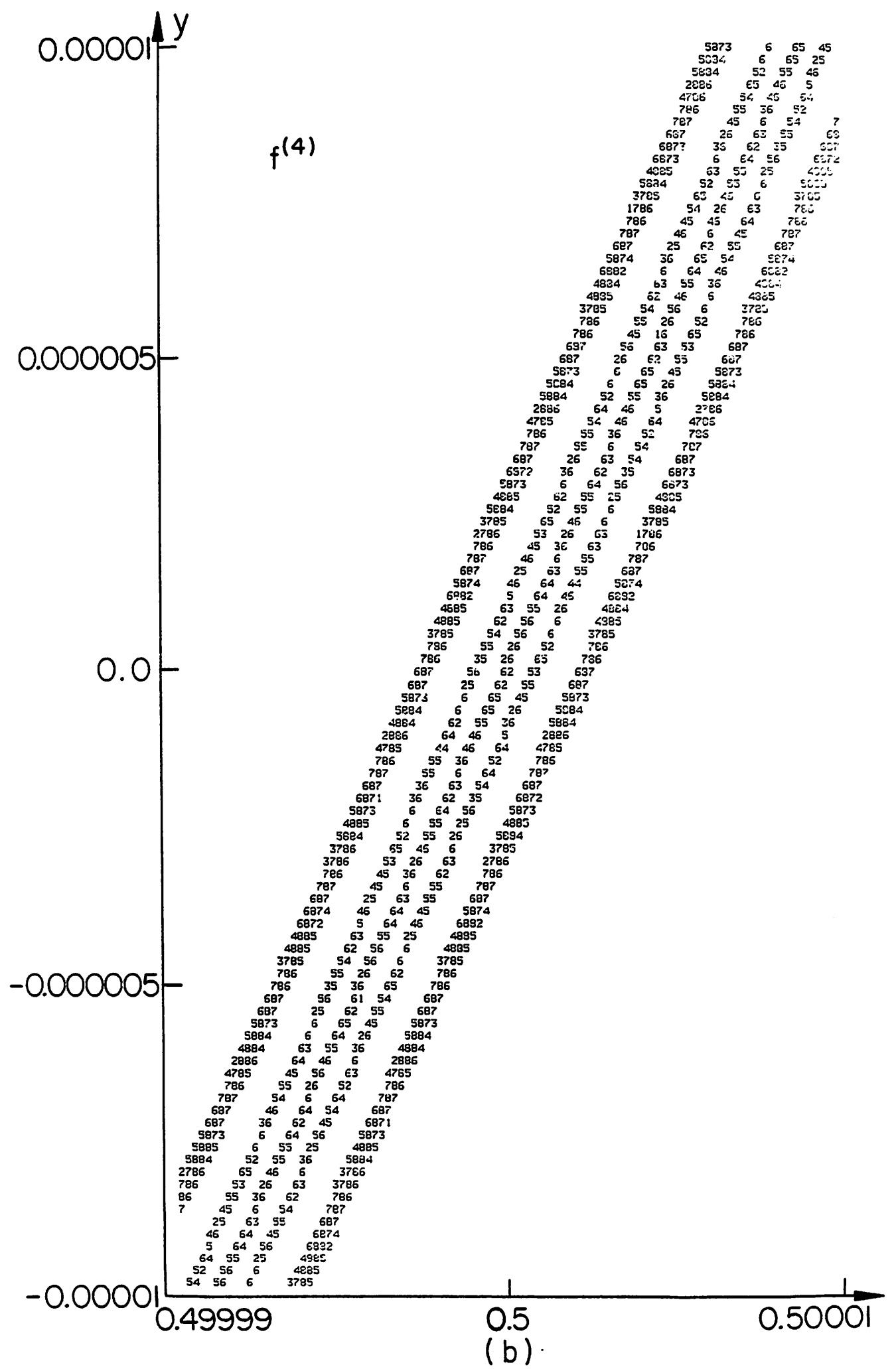


Fig. 4a





(b)